TRANSAT

Research and Innovation Action (RIA)

This project has received funding from the European Union's Horizon 2020 research and innovation programme under grant agreement No 754586.

Start date : 2017-09-01 Duration : 54 Months

Report on development of tools to study the environment fate of particles by-products

Authors : Mrs. Melanie AUFFAN (AMU), Danielle SLOMBERG (AMU-CEREGE), Jerome ROSE (AMU-CEREGE), Mickael Payet (IRSN)

TRANSAT - Contract Number: 754586

Project officer: Project Officer: Angelgiorgio IORIZZO

Document title	Report on development of tools to study the environment fate of particles by-products
Author(s)	Mrs. Melanie AUFFAN, Danielle SLOMBERG (AMU-CEREGE), Jerome ROSE (AMU-CEREGE), Mickael Payet (IRSN)
Number of pages	30
Document type	Deliverable
Work Package	WP03
Document number	D3.5
Issued by	AMU
Date of completion	2021-10-08 10:03:44
Dissemination level	Public

Summary

The present indoor freshwater mesocosm set-up and complementary batch experiments performed permit the analysis of the environmental fate and impact of both tritiated by-products and dissolved tritium. Our results highlight drastic differences in the contamination routes of a freshwater ecosystem and differences in the ecological niches potentially exposed to tritiated (3H) steel or cement particles released during dismantling. Indeed, the stainless steel particles were stable, but rapidly settled out of the water column. Only a small fraction of the tritium was released into the water column in the dissolved phase. The majority of the tritium remained bound to the steel particles residing in the surficial sediments. Benthic grazers appeared particularly sensitive to the stainless steel particles with significant behavioural changes observed. In the case of cement, there is an immediate dissolution of the particles, which will surely coincide with an important release of tritium in the water column. In that case we expect a more important exposure of the planktonic organisms to 3H. Freshwater indoor mesocosms appeared as well adapted experimental devices to quantitatively and qualitatively assess environmental dosimetry and the impacts of tritiated steel and cement particles likely released in aquatic ecosystems during dismantling.

Approval

Date	By
2021-10-08 17:18:46	Mrs. Veronique MALARD (CEA)
2021-10-11 14:02:56	Mr. Christian GRISOLIA (CEA)

DL. 3.5: Report on development of tools to study the environmental fate of particle by-products.

Deliverable:	**D3.5**
Work Package:	WP3
Due date of delivery:	According to DOA XX/XX/2021
Document status:	Draft
Submitted by:	
Lead author:	Slomberg Danielle (AMU-CEREGE)
Contributing authors	Auffan Mélanie (AMU-CEREGE), Rose Jérôme (AMU-CEREGE), Payet Mickaël (IRSN)

Document history

Version	Date	Who	Reason for change
1	30/09/2021	Danielle Slomberg, Melanie Auffan, Rose Jérôme (CEREGE)	First version
1	07/10/2021	Mickael Payet for the tritium lab in Saclay	Version validated without change

This project has received funding from the Euratom research and training programme 2014-2018 under the grant agreement n°754586. The content in this report reflects only the views of the authors. The European Commission is not responsible for any use that may be made of the information it contains.

Table of contents

TABLE OF FIGURES **3**

TABLE OF TABLES **4**

ABBREVIATIONS **4**

1 OBJECTIVES **5**

2 TOOL FOR STUDYING ENVIRONMENTAL FATE: AQUATIC MESOCOSMS **6**

2.1 AQUATIC MESOCOSM SET-UP 6
2.2 PARTICLE EXPOSURE SCENARIO 7
2.3 AQUATIC MESOCOSM MONITORING 7
2.4 ORGANISM VIABILITY AND BEHAVIOUR 7
2.5 TRITIUM AND SS316L PARTICLE QUANTIFICATION IN DIFFERENT ENVIRONMENTAL COMPARTMENTS 7

3 TRITIATED STAINLESS STEEL PARTICLE ENVIRONMENTAL FATE AND IMPACTS **8**

3.1 FAVORABLE BIO-PHYSICAL-CHEMICAL CONDITIONS DURING EXPOSURE IN FRESHWATER MESOCOSMS 8
3.2 LENTIC ECOSYSTEM EXPOSURE TO TRITIATED SS316L PARTICLES 9
3.2.1 Tracing of steel particles in complex environmental matrices 9
3.2.2 ^{3}H and SS316L partitioning between the water column and the surficial sediments 11
3.2.3 Homo-aggregation versus hetero-aggregation of tritiated steel particles 13
3.3 TRITIATED SS316L PARTICLES IMPACTS ON FRESHWATER ORGANISMS 14

4 CEMENT PARTICLE ENVIRONMENTAL FATE AND IMPACTS **16**

4.1 CEMENT PARTICLE STABILITY IN FRESHWATER 16
4.1.1 Cement particle elemental composition 16
4.1.2 pH evolution of cement particles in freshwater 18
4.1.3 Evolution of cement size distribution and particle number 19
4.1.4 Cement particle transformation and dissolution 20
4.2 ESTIMATED DISTRIBUTION IN DIFFERENT ENVIRONMENTAL COMPARTMENTS 24

5 CONCLUSIONS **25**

6 CITED REFERENCES **26**

7 ANNEXES **28**

Table of figures

Figure 1. Set-up of the freshwater indoor mesocosm experiments performed in the Tritium lab in Saclay (France) and the mesocosm facilities in Aix en Provence (France). 6
Figure 2. Evolution of the number of picoplancton in the water column and in the surficial sediment at 0 and 28 days. Water was samples at ~10cm from the air/water interface and sediment at less than 1mm depth. 9
Figure 3. Fe concentration in the surficial sediment (A), water column (B), and *A. leucostoma* (C) in control or H-SS316L exposed mesocosms over 4 weeks. Data between control and exposed mesocosms are not statistically different. 10
Figure 4. Dissolved concentrations (<3 KDa) of Mo, Mn, Ni, and Cr in the water columns of control and exposed mesocosms. Data between control and exposed mesocosms are not statistically different. Log-scale. 10
Figure 5. Total background concentrations of Fe, Mo, Mn, Ni, and Cr in the water columns, sediment and *A. leucostoma* of control. Log-scale. X-axis : days 11
Figure 6. Mo concentration as SS316L tracer in total water column and dissolved water column. ..12
Figure 7. Tritium concentration in (A) total water column and (B) dissolved water column. 12
Figure 8. Mo concentration (mg/kg) in surficial sediments and in the interstitial water of the control and H-SS316L exposed mesocosms. 13
Figure 9. ^{3}H concentration (Bq/mg) in surficial sediments and in the interstitial water in the H-SS316L and T-SS316L exposed mesocosms. 13
Figure 10. Number of suspended materials (0.2-1 µm and 1-10 µm) in uncontaminated water from control mesocosms and mesocosms contaminated with steel particles. X-axis: days 14
Figure 11. Concentration of Mo (ng/snail) and ^{3}H (Bq/snail) in rinsed *A. leucostoma* as well as the Mo concentration in the water used for the rinsing presented as ng of Mo per snail. 15
Figure 12. Fraction of the snails (% of the total population) displaying burrowing traits in controls and H-SS316L contaminated mesocosms. 16
Figure 13. pH evolution of 200 mg/L hydrogenated cement suspension in saline solution over 60 min. 18
Figure 14. pH evolution of H-cement suspensions in Volvic® water (1 and 10 mg/L) over 28 days (672 h). 19
Figure 15. Size distribution of 10 mg/L H-cement particles in Volvic® water at t0 and after 24h. ...19
Figure 16. A) Size distribution of 10 mg/L H-cement particles in Volvic® water at t0, 14d and 28d and (B) total number of particles per mL after 28 d. 20
Figure 17. Ca, Si, Al, and Ti concentrations in different fractions over time for 10 mg/L H-cement suspension prepared in Volvic® water. 21
Figure 18. % Ca calculated for the particulate (>0.2 µm), colloidal (0.002-0.2 µm), and soluble (<10kDa) fractions after aging in Volvic® water. 22
Figure 19. Ca, Si, Al, and Ti concentrations in different fractions over time for 10 mg/L H-cement suspension prepared in mesocosm water. 23
Figure 20. % Ca and Si calculated for the particulate (>0.2 µm), colloidal (0.002-0.2 µm), and soluble (<10kDa) fractions after aging in mesocosm water. 24

Figure A 1. Total and dissolved concentrations of Cr and Ni in water column. 28
Figure A 2. Total concentrations of Cr and Ni in surficial sediments and interstitial water. 29
Figure A 3. Total concentrations of Cr and Ni adsorbed to (left) and taken up in snails (right). 30

Table of tables

Table 1. Major element composition of cement particles determined using ICP-AES following an alkaline digestion. 17
Table 2. Trace element concentrations in cement particles determined using ICP-MS following acid digestion. 17
Table 3. Estimation of cement particle concentration that can be detected and quantified in Volvic® water, assuming all cement remains in water column. 18
Table 4. Estimation of cement particle concentration that can be detected and quantified in mesocosm surficial sediments, assuming all cement settles to sediment. 25
Table 5. Estimation of cement particle concentration that can be detected and quantified in A. leucostoma, assuming no cement transformation and comparable uptake to SS316L particles. 25

Abbreviations

EC DG RTD	European Commission – Directorate General for Research and Innovation
DoA	Description of Action
ECCP	Electronic Collaborative Content Platform
ExCom	Executive Committee
GB	Governing Board
PMO	Project Management Office
PQP	Project Quality Plan
PR	Periodic report
QA	Quality assurance
WP	Work package
WPL	Work package leader
SEM	Scanning Electron Microscope
XRD	X-ray Diffraction
HEPES	4-(2-hydroxyethyl)-1-piperazineethanesulfonic acid
MQ	Ultra-pure water
C-S-H	Calcium Silicate Hydrates (cement phase)
AFm	alumina, ferric oxide, monosulfate (cement phase)

This project has received funding from the Euratom research and training programme 2014-2018 under the grant agreement n°754586. The content in this report reflects only the views of the authors. The European Commission is not responsible for any use that may be made of the information it contains.

1 Objectives

This deliverable DL3.5 – Report on development of tools to study the environmental fate of particle by-products – is part of the work package 3 of TRANSAT. The main objective of work package 3 is to study the impact of tritiated products on environment and human health. One of the main actions of this work package 3 is the Action 2 that studies the environmental transformation of the released particle (steel and cement) by-products using mesocosm scale studies (AMU-CEREGE). More specifically we identified three main questions:

- What is the **major contamination route** of a freshwater ecosystem exposed to **tritiated (^{3}H) steel or cement particles** released during dismantling?
- Which **ecological niche** is most **exposed** and **sensitive** to dissolved ^{3}H or steel/cement particle-bound ^{3}H?
- What is the contribution of steel or cement particle-bound ^{3}H in terms of **dosimetry** and **environmental impact**?

To answer these questions, we used freshwater indoor mesocosms. Mesocosm testing offers a means of providing meaningful data to inform environmental risk assessment of complex systems (Auffan et al., 2014, 2019). Among the many definitions for a mesocosm, a more general one describes a mesocosm as an enclosed and essentially self-sufficient (but not necessarily isolated) experimental environment or ecosystem with a number of interdependent system parameters.

The mesocosms used herein were developed by AMU-CEREGE as a Standard Operational Procedure for pre-regulatory purposes in environmental nanosafety during the NanoREG EU project (FP7 Grant Agreement n.310584). This method consists of monitoring the evolution of a re-created miniature ecosystem following nanoparticle contamination and environmental aging (Masion et al., 2019). The only decision in this risk assessment strategy is the definition of an environmentally relevant exposure scenario (incl. dose). Such a robust testing strategy (Nassar et al., 2021) bears clear advantages for the determination of both (nano)particle/tritium exposure and hazard in a single experiment (Tella et al., 2014, 2015; Auffan et al., 2018, 2020; Chatel et al., 2020), and for producing dependable and intercomparable data (Nassar et al., 2020; Ayadi et al., 2021).

2 Tool for studying environmental fate: Aquatic mesocosms

2.1 Aquatic mesocosm set-up

For each experiment, four indoor aquatic mesocosms (glass tanks of 350 × 200 × 400 mm) were set up to mimic a natural pond ecosystem. The organisms selected for this study were picoplankton and picobenthos primary producers (e.g., bacteria, algae, protozoa from natural inoculum) sampled from a non-contaminated pond in the South of France (N 43°20′47.04″, E 6°15′34.786″), as well as the benthic grazing snail, *Anisus leucostoma* (*A. leucostoma)*, also sampled from the same non-contaminated pond. Each mesocosm consisted of a bottom layer of ~ 2.3 kg artificial sediment (89% SiO_2, 10% kaolinite, and 1% $CaCO_3$) covered by 150 g of water-saturated natural sediment containing primary producers (sieved at 250 µm), followed by 16 L of Volvic® water, which has pH and conductivity values close to those of the natural pond water. Picoplankton recovered from the natural pond surface water were also added to the mesocosm. Briefly, 100 mL of pond water was sieved (250 µm), then successively filtered at 2 µm and 0.2 µm. The 0.2 µm filter was then recovered and agitated in 100 mL Volvic® water to resuspend the picoplankton, and 40 mL of this water inoculum was injected into each mesocosm. A day/night cycle of 6 h/18 h was applied using full spectrum light (Viva® light T8 tubes 18 W), and the room temperature was kept constant at 16°C. The mesocosm experiments were performed under static conditions. Ultrapure water was added to the mesocosms weekly to compensate for evaporation. Two weeks of equilibration were necessary for the stabilization of the mesocosm physico-chemical parameters and the development of the primary producers. Then, ~20 adult *A. leucostoma* (6.0 ± 0.6 cm diameter) were introduced per mesocosm and acclimatized for 3 days prior to starting the experiment.

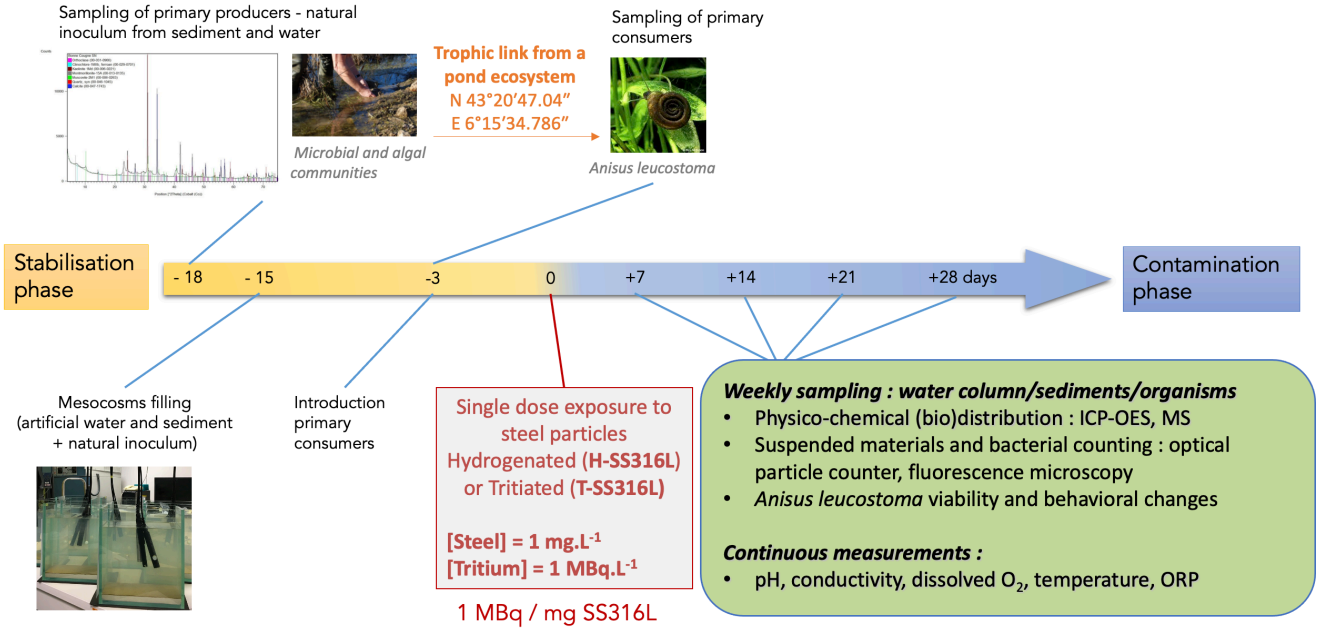

Figure 1. Set-up of the freshwater indoor mesocosm experiments performed in the Tritium lab in Saclay (France) and the mesocosm facilities in Aix en Provence (France).

2.2 Particle exposure scenario

The aquatic mesocosm experiments were designed to simulate a one-time contamination of a pond ecosystem under static conditions to tritiated steel particles. Stainless steel fate and behaviour in the mesocosms was monitored at the CEREGE using surrogate hydrogenated stainless steel particles (H-SS316L), while tritium distribution in the different environmental compartments was determined using tritiated stainless steel particles (T-SS316L) in a parallel experiment conducted at the Saclay tritium lab. Please see deliverables D3.2 and D3.3 for details on the production, characterization and hydrogentation/tritiation of the ~ 3 µm hydrogenated and tritiated stainless steel particles. The one-time contamination was performed by injecting 16 mL of a suspension (in ultrapure water) containing 16 mg of H-SS316L or T-SS316L for a final concentration of 1 mg/L stainless steel particles in the mesocosm water column. In the case of the T-SS316L exposure, the injection of 1 mg/L T-SS316L corresponded to a tritium concentration of 1 MBq/L i.e. 1 MBq per mg of SS316L.

2.3 Aquatic mesocosm monitoring

For each mesocosm, multiparameter probes (Odeon® Open X) were installed to monitor the temperature, pH, redox potential, and dissolved O_2 in the water column for the entire duration of the experiment. The number of colloidal particles suspended in the water column was monitored weekly at 10 cm below the water surface using an optical particle counter (Flowcell FC200S + HR, Occhio, Belgium). Particles with sizes ranging from 0.2 to 52 µm in the water column were considered.

2.4 Organism viability and behaviour

Picoplankton (cells between 0.2 to 2 µm) concentrations were determined at the surface of the sediment (0.5 ± 0.1 mm depth) and in the water column (10 cm below the air-water interface) on a weekly basis. To determine picoplankton concentrations, water (10 mL) and sediment (15 mL) were sampled at Days 0 and 28, treated with formaldehyde (3.7%), and stored at 4°C until counting. Counting was performed by mixing 10 µL of each sample with 5 µL 3 µM SYTO® 9 Green Fluorescent Nucleic Acid Stain on a glass slide and observing the number of cells in five different zones using a fluorescence microscope. The concentration of picoplankton (cells/mL) was reported as the mean ± standard deviation of the five different zones. The benthic grazing snail, *A. leucostoma*, was observed weekly for viability and localization within the mesocosm (i.e., at the water surface or in the sediment) as an indication of potential behavioral changes.

2.5 Tritium and SS316L particle quantification in different environmental compartments

The tritium and the SS316L particle distributions in the mesocosms were quantified by respectively measuring the tritium and main metals (i.e., Fe, Cr, Ni, Mo, Mn) present in steel ,in the surficial sediments, water column, and the *A. leucostoma* organisms. Sampling was performed weekly over 4 weeks. The surface sediments were sampled at three different locations and pooled before drying

24 h at 50 °C. The water column was sampled at 10 cm below the surface of the water. The soluble fraction of tritium and metals in the water column was also determined by using Amicon® Ultra-4 3 K centrifugal filter devices (3 000MWCO, size retention limit ~ 1 nm, Merck-Millipore) by centrifuging aliquots of surface water at 4000*g* for 1 h to separate the soluble and particulate fractions. Ten *A. leucostoma* were sampled at weeks 2 and 4, rinsed with clean Volvic® water (3 mL), and stored after drying 24 h at 50 °C. Before elemental analysis, the water column and *A. leucostoma* rinse samples (2 mL) were acid-digested at ambient temperature (3 mL HCl 37% Normatom® + 1 mL HNO_3 65% Normatom®) for 48 h. Sediment and *A. leucostoma* samples were first ground using a mortar and pestle, then acid-digested prior to tritium analysis or mineralized at 180°C by using a microwave digestion system (ultraWAVE, Milestone, Italy) prior to elemental analysis. For elemental analysis of sediment samples (50 mg), a mixture of 3 acids (1.5 mL HCl 37% (Normatom®), 1 mL HNO_3 65%, 1 mL of HF 47%-51%) was used, while *A. leucostoma* organisms (50 mg) were digested in 1 mL HCl 37%, 1 mL HNO_3 65%, 1 mL H_2O_2 30%-32% (PlasmaPure®) and 0.5 mL HF 47%-51%. Concerning the radioactivity (i.e., tritium) measurements, beta counting was performed on samples from each mesocosm compartment, either directly (water) or after drying, grinding, and acid digestion (surficial sediments and *A. leucostoma*).

3 Tritiated stainless steel particle environmental fate and impacts

3.1 Favorable bio-physical-chemical conditions during exposure in freshwater mesocosms

The mesocosms were contaminated with a one-time injection of H-SS316L or T-SS316L particles and monitored over 28 days. During this phase, several physical-chemical and microbial parameters were monitored to assess the global response of the mesocosms to the presence of the SS316L particles. Physical-chemical parameters monitored on the field the day of sampling were: temperature (5 °C), dissolved O_2 (66 %, 8.6 mg/L), conductivity (430 µS/cm), and pH (8.1). Physical-chemical parameters monitored during the whole experiment were constant during the contamination period: temperature (15.8 ± 0.8 °C), dissolved O_2 (80−93 %), redox potential (414 ± 72 mV), conductivity (300 ± 4 µS/cm), and pH (7.6 ± 0.2). On the whole, no significant differences were observed between control and contaminated mesocosms, nor between the mesocosms and the field conditions (with the exception of the temperature).

The number of picoplankton (cells between 0.2 and 2 µm) was measured in the water column and surficial sediments at Days 0 and 28. The total number of cells remained constant over time, i.e. ~10^6 cells.mL^{-1} in the surficial sediment and between 10^4 and 10^5 cells.mL^{-1} in the water column, with no significant differences in the picoplankton number observed between the control and contaminated mesocosms.

Finally, the ecological conditions of the mesocosms remained favorable during the exposure to H-SS316L and T-SS316L with oxygenation, pH, temperature, redox potential, and the number of

primary producers all in the range of natural conditions. This is consistent with the scenario of exposure selected, which has been found to be acutely non-toxic for the ecosystem mimicked (e.g. Tella et al., 2014, 2015; Auffan et al., 2018, 2020; Chatel et al., 2020).

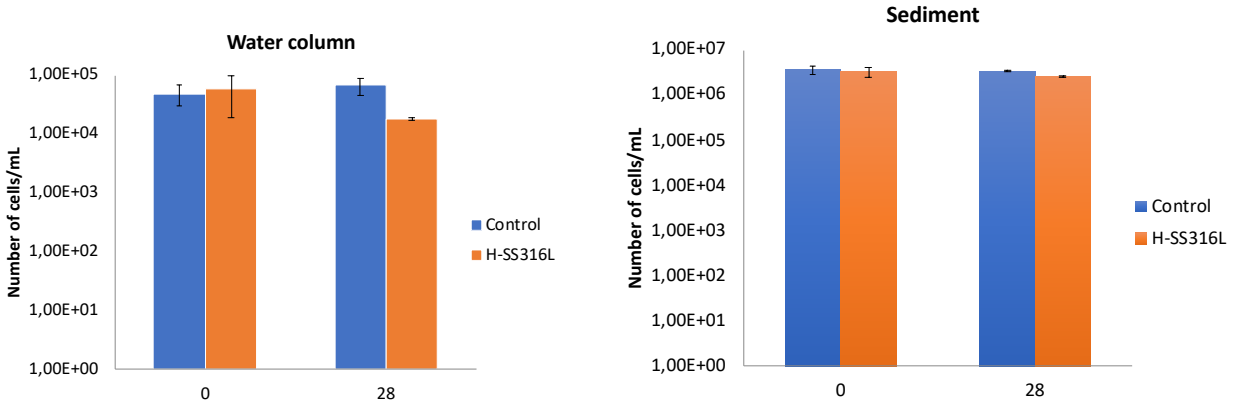

Figure 2. Evolution of the number of picoplancton in the water column and in the surficial sediment at 0 and 28 days. Water was samples at ~10cm from the air/water interface and sediment at less than 1mm depth.

3.2 Lentic ecosystem exposure to tritiated SS316L particles

3.2.1 Tracing of steel particles in complex environmental matrices

Despite the fact that Fe represents 69 wt% of the SS316L, the elevated background in the mesocosm compartments (surficial sediment, water column, and primary consumers) makes its use as a tracer of the SS316L particles challenging. As shown in Figure 3, the concentrations of Fe obtained in the water, sediment, and *A. leucostoma* were never significantly different from the controls. Consequently, the dosing of Fe as a tracer of SS316L was not an option.

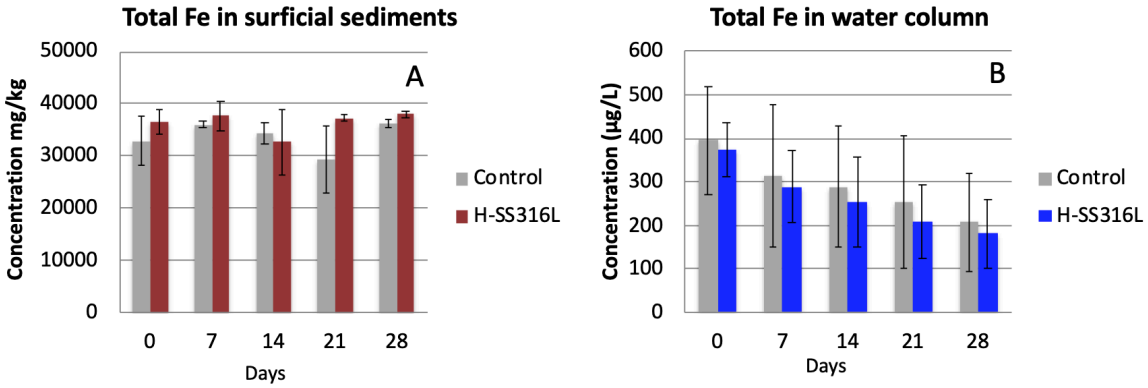

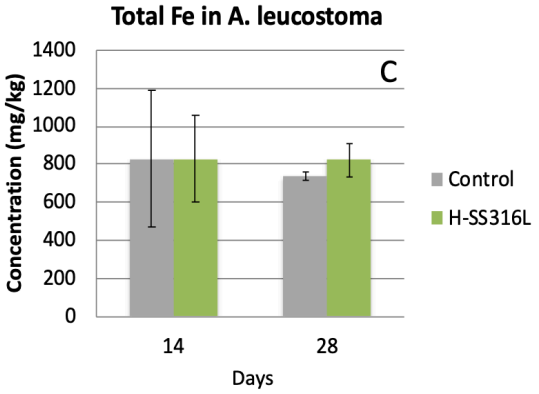

Figure 3. Fe concentration in the surficial sediment (A), water column (B), and *A. leucostoma* (C) in control or H-SS316L exposed mesocosms over 4 weeks. Data between control and exposed mesocosms are not statistically different.

To get around this analytical issue, the possibility of using Cr (17 wt% of SS316L), Mo (2 wt% of SS316L), Ni (10 wt% of SS316L), and Mn (1 wt% of SS316L) as SS3316L tracers was assessed. First, we ensured that Cr, Mo, Ni, and Mn did not dissolve in the water column of the different mesocosms over the course of the 28 d contamination phase (Figure 4). Second, we ensured that the background concentrations of these elements were low compared to Fe in the water column, sediment, and *A. leucostoma* (Figure 5). Based on these requirements and on the results obtained, we selected Cr, Mo, and Ni as relevant tracers of SS316L in the mesocosms. For reasons of clarity, only the data associated with using Mo as a SS316L tracer will be presented in this deliverable, however results using Cr and Ni were comparable and support the same conclusions (Annexe Figures A1-A3).

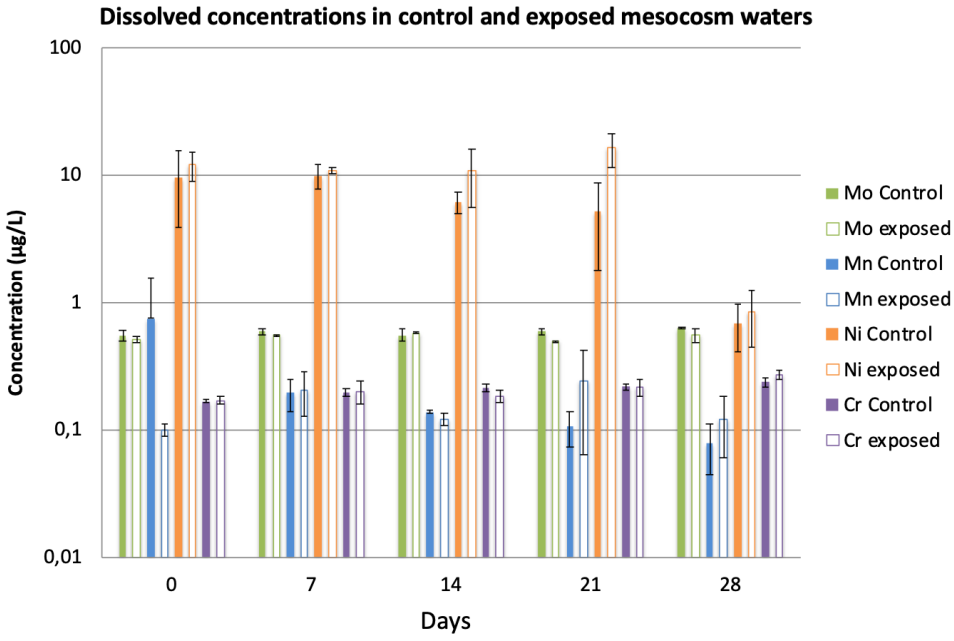

Figure 4. Dissolved concentrations (<3 KDa) of Mo, Mn, Ni, and Cr in the water columns of control and exposed mesocosms. Data between control and exposed mesocosms are not statistically different. Log-scale.

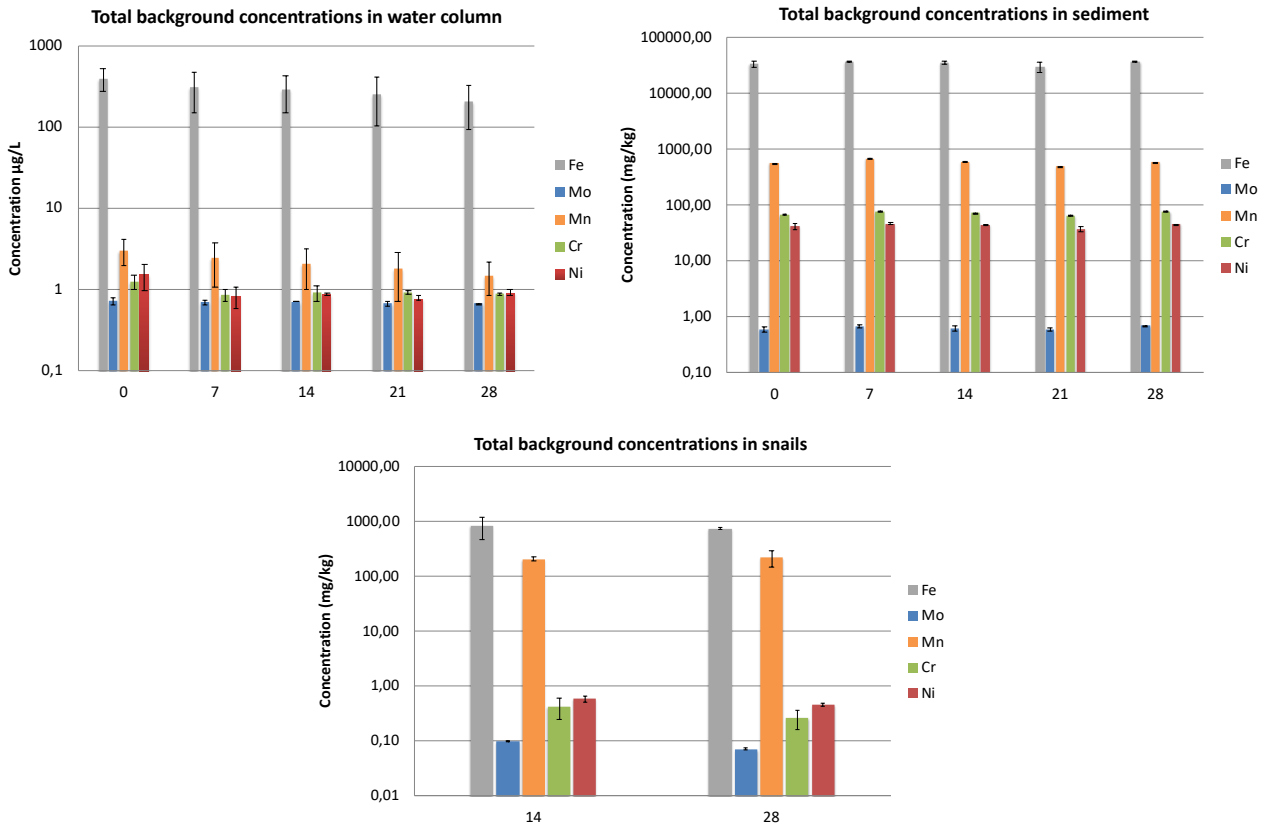

Figure 5. Total background concentrations of Fe, Mo, Mn, Ni, and Cr in the water columns, sediment and *A. leucostoma* of control. Log-scale. X-axis : days

3.2.2 ^{3}H and SS316L partitioning between the water column and the surficial sediments

Water and sediment samples were collected at days 0, 7, 14, 21 and 28. Water was sampled at ~10 cm from the air/water interface. Surficial sediments were sampled at three different locations and then pooled before being dried. It was estimated that sediment sampling mainly affected the first 500 µm – 1000 µm below the water /sediment interface.

Figure 6 shows the Mo concentrations (tracer of SS316L particles) measured in the water column as a function of time. No significant increase in the total Mo concentration nor the dissolved Mo concentration could be evidenced in the water column of mesocosms contaminated with H-SS316L during one month. This highlights the fast kinetics of removal of the SS316L particles that occurred during the first week. These results are also consistent with the slow dissolution kinetics of SS316L.

Figure 7 gives the tritium concentration in the water column following exposure to the T-SS316L. Seven days after contamination a significant concentration of tritium was dosed in the water column which remained stable over time. The ~150 Bq/mL dosed in the water column corresponded to 16 ± 2 % of the total tritium injected. To identify whether the tritium was bound to particles (SS316L or natural suspended particles) or dissolved, ^{3}H dosing was also performed after ultrafiltration of the

water at 3 KDa. The similar tritium concentrations measured before and after ultrafiltration allow us to conclude that the tritium measured in the water column of the mesocosms was fully dissolved.

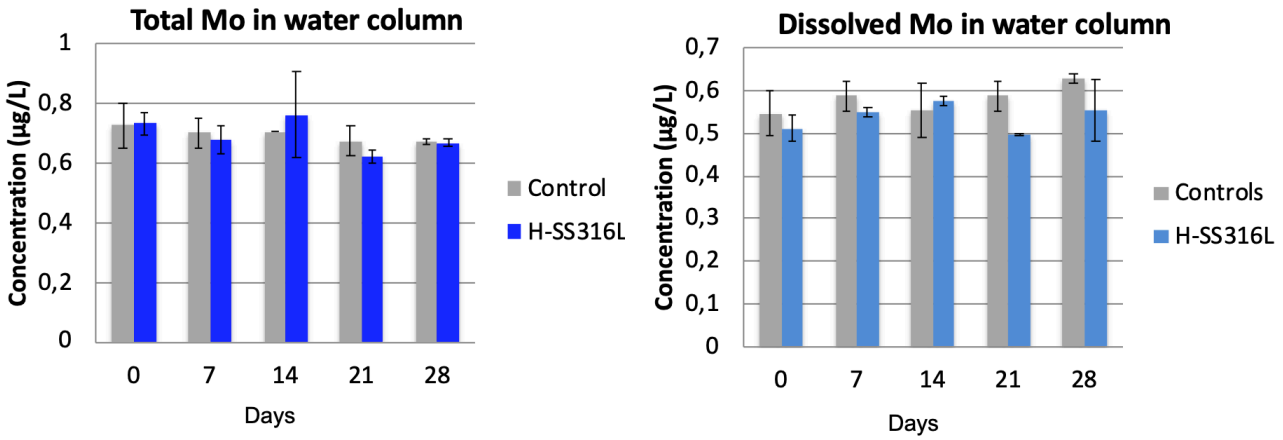

Figure 6. Mo concentration as SS316L tracer in total water column and dissolved water column.

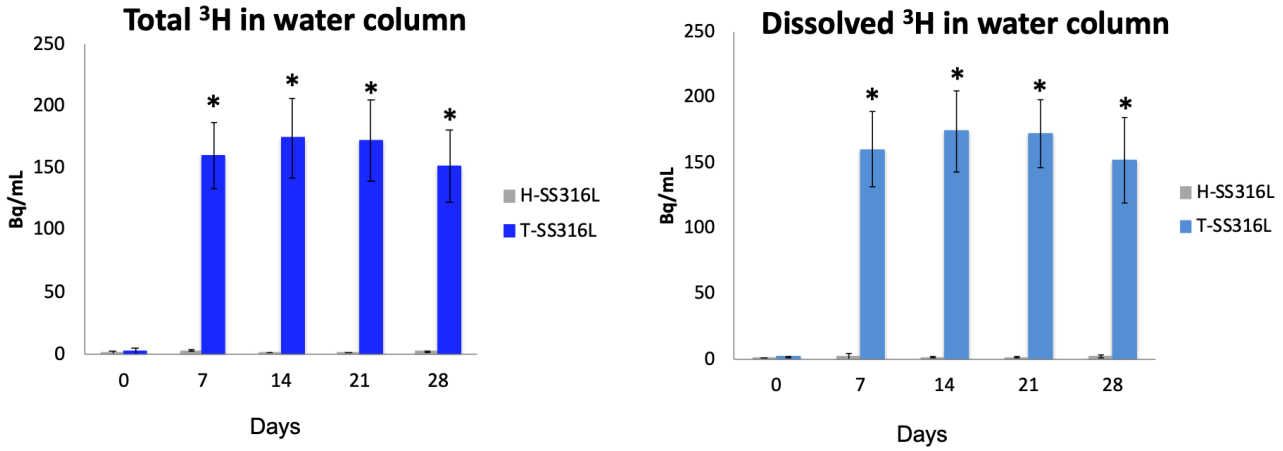

Figure 7. Tritium concentration in (A) total water column and (B) dissolved water column.

In Figure 8, the Mo concentrations determined in surficial sediment and in its interstitial water were plotted. Despite the large variability attributed to sampling heterogeneity, significant differences in the Mo concentrations measured in the sediment were observed compared to the control at each sampling time. Concentrations averaging between 19 ± 6 mg Mo/kg sediment (day 7) and 10 ± 2 mg Mo/kg sediment (day 14, 21, and 28) were measured. Given these concentrations, we estimated that at the end of the experiment, 132 ± 37 % of the total SS316L had settled down in the surficial sediment. Regarding the tritium concentration in the benthic compartment, Figure 9 highlights that ^{3}H in surficial sediment reach 409 ± 12 Bq/mg of sediment after 28 days. The interstitial concentration of ^{3}H was also measured and the results (~ 150 Bq/mL) obtained at each sampling time indicated that the interstitial water is in equilibrium with the water column.

Two hypotheses can be supported by these results: 1) the tritium found in the sediment is still bound to the SS316L particles, 2) the tritium in the sediment has been first released from the SS316L particles and then adsorbed at the surface of inorganic or organic phases of the sediment. Assuming that after 28 days in the surficial sediment, all the ^{3}H (409 ± 12 Bq/mg of sediment) is still bound to the SS316L (10 ± 2 mg Mo/kg of sediment), this leads to an expected activity of the particles of 0.84 ± 0.2 MBq / mg of SS316L. This value is very close to the 1.0 ± 0.1 MBq / mg of SS316L calculated from our measurements and is in favour of the first hypothesis. All these results highlight that the surficial sediments concentrate the pollution and will be an important sink of tritiated particles potentially released during dismantling of a nuclear power plant.

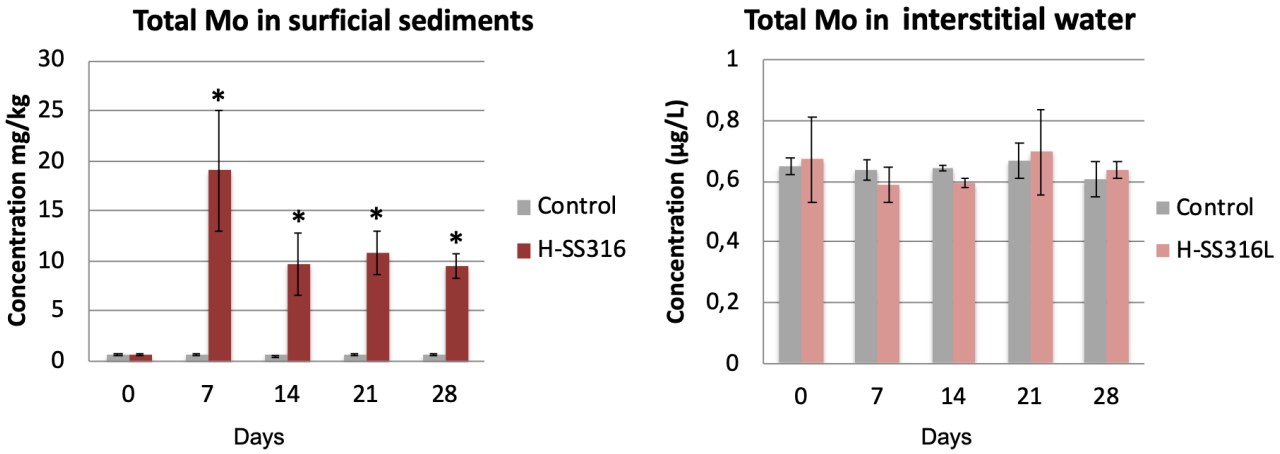

Figure 8. Mo concentration (mg/kg) in surficial sediments and in the interstitial water of the control and H-SS316L exposed mesocosms.

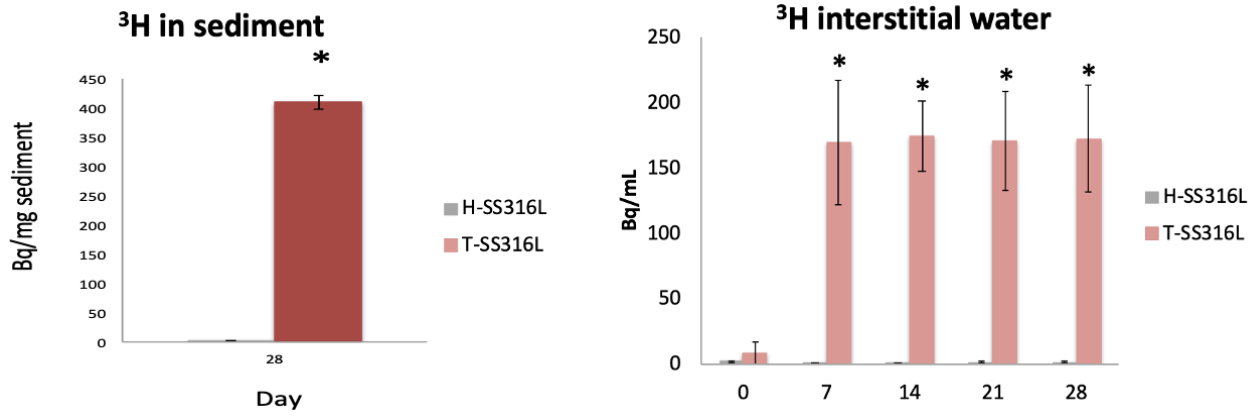

Figure 9. ^{3}H concentration (Bq/mg) in surficial sediments and in the interstitial water in the H-SS316L and T-SS316L exposed mesocosms.

3.2.3 Homo-aggregation versus hetero-aggregation of tritiated steel particles

Two mechanisms can be involved in the settling of the SS316L particles at the surface of the sediment: homo-aggregation and/or hetero-aggregation with natural colloids. Indeed, natural colloids

present in the mesocosms water (e.g. suspended clays, natural organic matter) can cause the settling down of hetero-aggregates of colloids and steel particles. In the mesocosm water, the number of colloids in the 0.2-1 µm fraction (mostly kaolinite clay) was close to 10^5 particles/mL (Figure 10). No significant differences of the number of colloids were observed after steel particle injection, indicating that hetero-aggregation was not detectable in these experimental conditions.

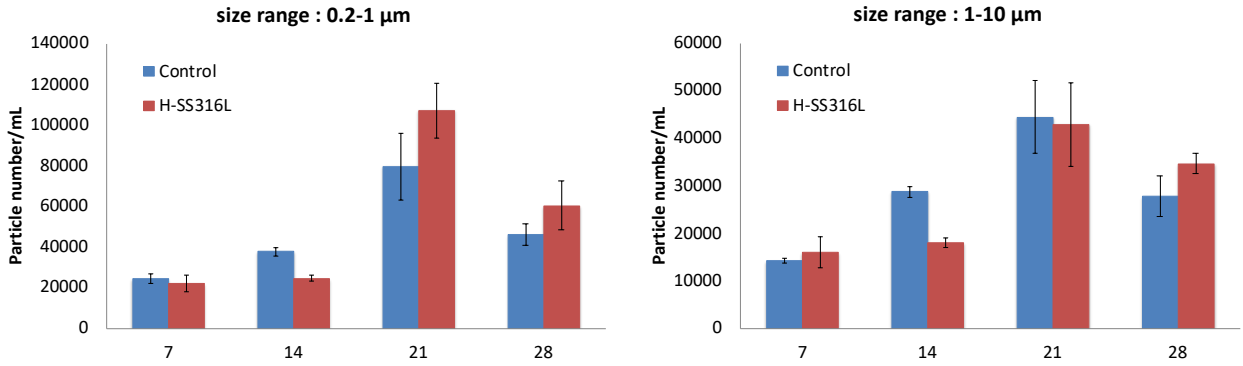

Figure 10. Number of suspended materials (0.2-1 µm and 1-10 µm) in uncontaminated water from control mesocosms and mesocosms contaminated with steel particles. X-axis: days

Moreover, because of the pH and ionic strength of the mesocosms water column, SS316L particles are colloidally unstable and will likely homo-aggregate. Using the Stokes' law :

$$v = \frac{2}{9}\frac{(\rho_p - \rho_f)}{\mu} g R^2$$

*with v the velocity (m/s), g the gravitational field strength (m/s^2), R the radius of the spherical particle (m), ρ_p the mass density of the particle (kg/m^3), ρ_f the mass density of the fluid (kg/m^3), and µ the viscosity (kg/(m*s))*

we estimated that about 30 minutes will be necessary for the SS316L particles to settle. The undetectable change in natural colloids number associated with the fast kinetics of settling down, led to the conclusion that homo-aggregation in the most favourable mechanism of steel particles partitioning in the mesocosms. In addition, the ~6 µm steel particles were not detected in the 1-10 µm particle fraction during the experiment further supporting their fast kinetics of settling down.

3.3 Tritiated SS316L particles impacts on freshwater organisms

A. leucostoma are benthic grazers that eat algae and biofilms at the sediment/water interface. Since the tritiated steel particles are concentrated in the sediment, these benthic grazers live and feed in a sensitive ecological niche. The uptake of Mo from SS316L particles was estimated at 7, 14, 21 and 28 days by (i) rinsing the snails and analysing the rinse water, and (ii) by analysing the rinsed snails. Moreover, the amount of ^{3}H taken up by the snails (rinsed snails) was measured after 28 days of exposure. Figure 11 shows that a significant amount of Mo was measured in the water used to rinse

the snails. This corresponds to ~0.8 ng of Mo per snail that is likely adsorbed on the shell. Significant concentrations of Mo (~1.5 ng of Mo/snail) and ^{3}H (~35 Bq/snail) were also measured after snail rinsing. These concentrations correspond to <0.01% of ^{3}H and <0.01% of SS316L initially injected. Based on the feeding regimen of the snails and on previous mesocosm experiments performed with TiO_2, CuO and CeO_2 nanoparticles, it is likely that the SS316L and ^{3}H are localized in the digestive gland of *A. leucostoma* (Tella et al., 2014, 2015; Auffan et al., 2018; Chatel et al., 2020).

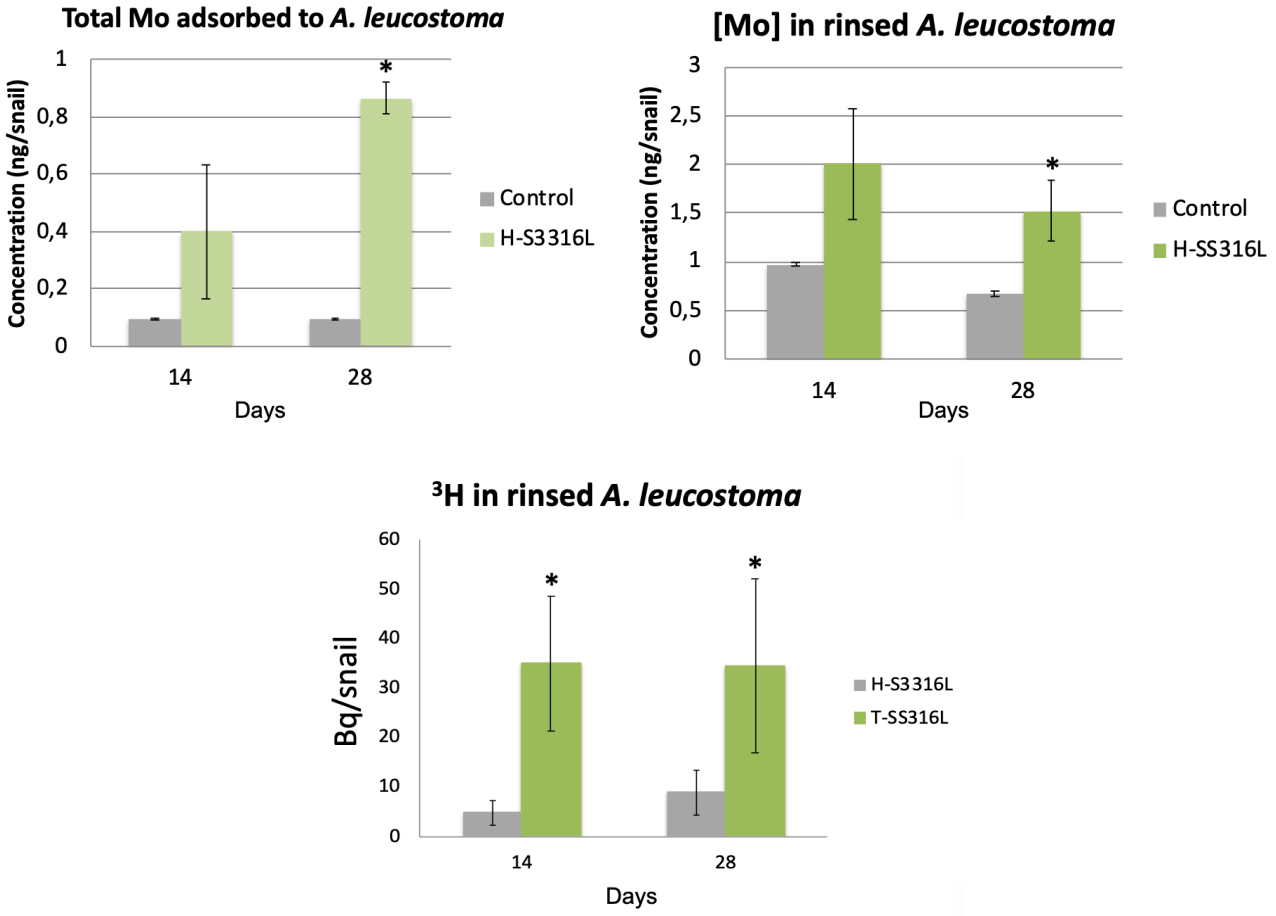

Figure 11. Concentration of Mo (ng/snail) and ^{3}H (Bq/snail) in rinsed *A. leucostoma* as well as the Mo concentration in the water used for the rinsing presented as ng of Mo per snail.

Following the adsorption of H-SS316L on the shell and their potential ingestion, the survival rate of *A. leucostoma* (<1% of mortality) was not affected. It is noteworthy that no acute toxicity was observed over the one-month experiment, neither for the primary consumers nor the primary producers (Figure 2). Aquatic organisms can respond to stress with a combination of physiological adaptation and behavioural responses (MacInnes and Thurberg, 1973). Herein, we noticed that the snail behaviour was affected following exposure to H-SS316L (increased burrowing activity and time spent in sediment). These different behaviours in sediment were observed after 18 and 21 days of exposure and were significantly different from controls (Figure 12). In freshwater aquatic snails, variation in living traits in sediment such as burrowing activity could have several implications in the

ecology, population dynamics and habitat features of a species (Lillebø et al., 1999). Nevertheless, a thorough characterization of the biological responses in the presence of tritiated SS316L is still required. Indeed, with mixtures (as in tritiated particles), we could observe additive effects (which results in the sum of toxicity of each agent), synergistic effects (inducing toxic effects greater than the sum of the effects of the individual chemicals) or also antagonistic effects (where the combined effect of two or more compounds is less toxic than the individual effects) (Roell et al., 2017). The potential joint radiotoxicity (due to ^{3}H) and particle toxicity (due to SS316L particles) needs to be further understood.

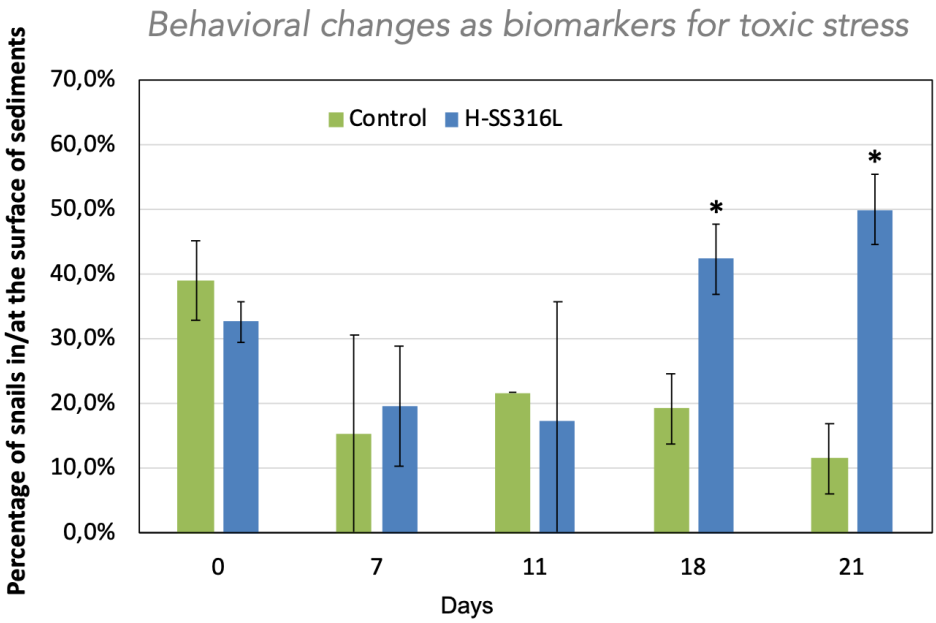

Figure 12. Fraction of the snails (% of the total population) displaying burrowing traits in controls and H-SS316L contaminated mesocosms.

4 Cement particle environmental fate and impacts

4.1 Cement particle stability in freshwater

4.1.1 Cement particle elemental composition

Cement particles in the 1−10 µm size range were produced according to the procedure reported in DL 3.2. For initial investigations, surrogate, non-radioactive hydrogenated particles (ambient temperature, 0.2 bar, 24h) were analysed for their physical-chemical stability and fate in freshwater systems.

The 1−10 µm hydrogenated cement particles (H-cement) were first characterised for their elemental composition. The weight % composition of the major elements (Ca, Si, Al, and Ti) was determined after an alkaline digestion and analysis using inductively coupled plasma-atomic emission spectroscopy (ICP-AES) (Table 1). While this alkaline digestion protocol offers the best elemental

recovery for cement, it was not optimal for use by other project partners due to the specialized equipment necessary and low sample throughput. We therefore proceeded with an acid digestion protocol at ambient temperature similar to that developed for the SS316L particles. Briefly, 1 mL of liquid sample containing the cement particles was acid digested (3 mL HCl 37% Normatom® + 1 mL HNO_3 65% Normatom®) at ambient temperature for 24 h. The aforementioned acid digestion resulted in lower recoveries for some of the major elements (i.e., 100% Ca, ~60% Si, 80-85% Al, and 5% Ti recovery). Based on these results, Ti was eliminated as a suitable tracer for cement particles in the environmental matrices. Trace elemental concentrations in the cement particles were also determined following acid digestion and analysis with ICP-MS, as shown in Table 2.

Table 1. Major element composition of cement particles determined using ICP-AES following an alkaline digestion.

	wt%
Ca	46.6
Si	10.8
Al	2.7
Ti	1.7

Table 2. Trace element concentrations in cement particles determined using ICP-MS following acid digestion.

	Se	Sr	Pb	Hg	Cr	Ni	Cu	Zn	As	Cd	Sb
wt%	<LD	0.09	0.003	<LD	0.01	0.006	0.02	0.01	0.01	0.001	0.001
mg/kg	<LD	882	33.7	<LD	100	58.4	205	114	114	9.3	5.8

An added difficulty in tracking cement particles in a lentic ecosystem is that the main elements of cement (i.e., Ca, Si, Al, and Ti) also have elevated environmental background concentrations. Using the known cement and Volvic® water elemental compositions, we were able to estimate the lowest cement particle concentration that can be detected in Volvic® water, the representative freshwater used in our studies (Table 3). Unlike for the SS316L particles, the cement particles cannot be dosed at 1 mg/L. However, at 10 mg/L cement particles, elements such as Ca, Si, Ti and Cr are likely to be measured apart from the Volvic® water background. As such, it was decided that the experiments evaluating cement stability and transformation in freshwater would be conducted at a concentration of 10 mg/L, following dilution from an appropriate stock solution.

Table 3. Estimation of cement particle concentration that can be detected and quantified in Volvic® water, assuming all cement remains in water column.

Element	Background in water (ug/L)	1 mg/L cement addition (ug/L)	Detection possible?	10 mg/L cement addition (ug/L)	Detection possible?
Ca	26560 ± 146	465	X	4645.5	Yes
Si	9384 ± 237	108	X	1084.5	Yes
Al	309 ± 365	27.0	X	270	X
Ti	19 ± 17	17.4	X	174	Yes
Fe	133 ± 143	2.1	X	21.25	X
Cr	0.42 ± 0.25	0.067	X	0.67	Yes

4.1.2 pH evolution of cement particles in freshwater

As detailed in DL 3.2, cement suspensions in water have a high pH buffer capacity at the concentration (2 g/L) targeted for stock suspension preparation. The high pH of the 2 g/L suspension would create strong chemical stress and lead to very high toxic effects, as well as particle dissolution. Therefore, the cement particles were first suspended in a buffered saline solution (0.9% NaCl, 1.25 mM $CaCl_2$, 10 mM HEPES) at 200 mg/L. The addition of the cement particles immediately increased the pH of the saline solution from ~ pH 7 to 7.6, after which the pH remained relatively stable up to 60 minutes after preparation (Figure 13). The pH of this suspension remained in an acceptable range (i.e., pH < 8) for experiments in environmental media, so it was decided that a 200 mg/L cement suspension in saline solution would be prepared and immediately used to make dilutions in Volvic® water for experiments on cement particle stability in freshwater systems.

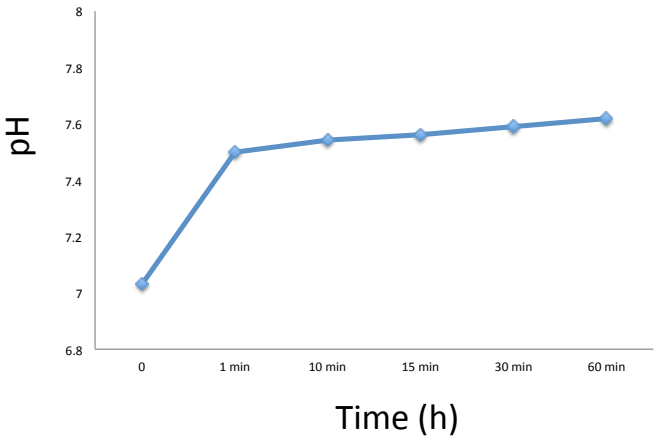

Figure 13. pH evolution of 200 mg/L hydrogenated cement suspension in saline solution over 60 min.

The pH evolution was then evaluated at 1 and 10 mg/L H-cement in Volvic® water. The initial pH of the Volvic® water was ~7.5. After addition of the cement particles using the 200 mg/L suspension in saline to reach a final concentration of 1 or 10 mg/L in Volvic® water, the pH slowly increased, reaching a maximum of pH ~7.8−7.9 after 168 h (14 d) as shown in Figure 14. The pH of both the 1 and 10 mg/L H-cement suspensions then remained more or less stable throughout the rest of the

672 h (28 d) experiment. As the pH remained < 8 over the duration of the experiment, it is expected that cement particles at 1 and 10 mg/L will not lead to toxic effects related to changes in pH.

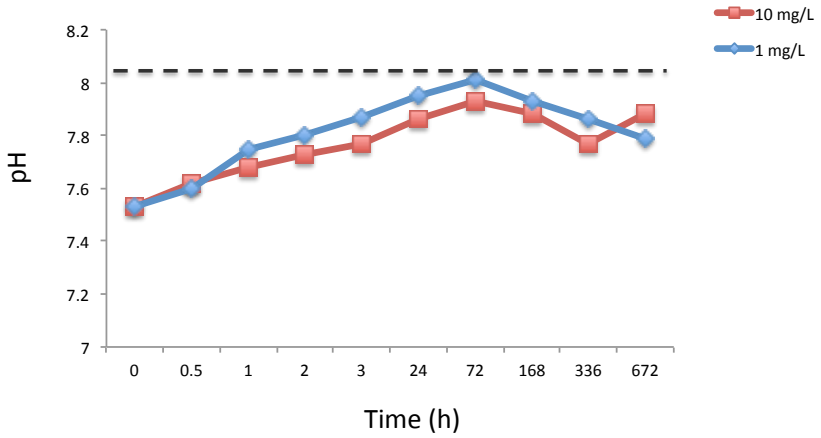

Figure 14. pH evolution of H-cement suspensions in Volvic® water (1 and 10 mg/L) over 28 days (672 h).

4.1.3 Evolution of cement size distribution and particle number

Another way in which the cement particle stability was assessed was by monitoring the particle size distribution and the number of particles in suspension using an optical particle counter (Flowcell FC200S + HR, Occhio, Belgium). The hydrodynamic diameter of the main H-cement peak was ~1.6−1.9 µm in Volvic® water and no significant change in the size distribution or particle number was observed over 24h (Figure 15). However, after 14d and 28d in the Volvic® water, there was a significant increase in the number of small particles (0.2−1 µm) and the total number of particles. The number of small particles in the 0.2−1 µm fraction increased from 52% to 61% of the total after 28d (Figure 16A), while the total number of particles doubled (Figure 16B). This suggests a transformation of the cement particles after 14-28 d aging in Volvic® water, with the release of nano-sized by-products.

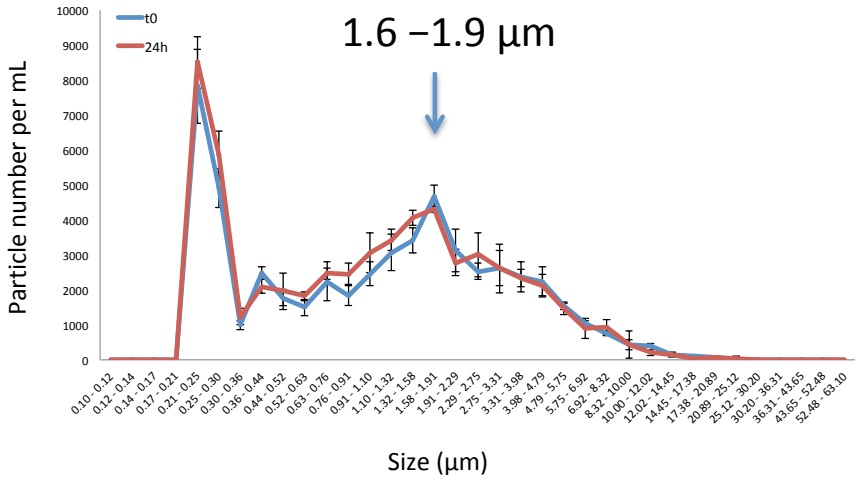

Figure 15. Size distribution of 10 mg/L H-cement particles in Volvic® water at t0 and after 24h.

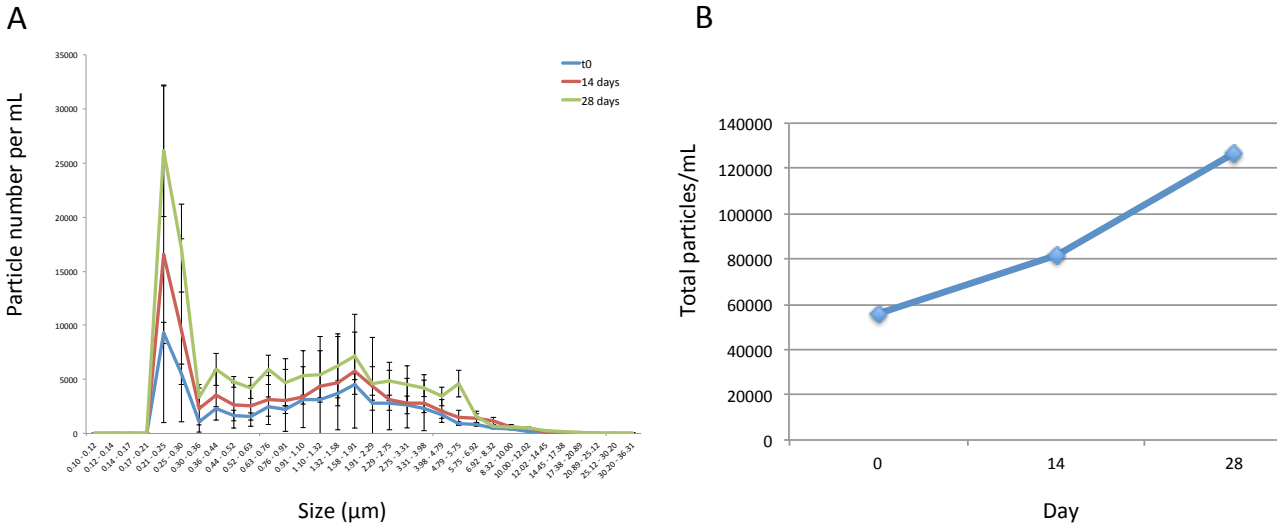

Figure 16. A) Size distribution of 10 mg/L H-cement particles in Volvic® water at t0, 14d and 28d and (B) total number of particles per mL after 28 d.

4.1.4 Cement particle transformation and dissolution

To further investigate particle transformation and any potential dissolution, a H-cement suspension was prepared at 10 mg/L in Volvic® water, and an aliquot was immediately sampled to determine the concentrations of the major elements (Ca, Si, Al, Ti) in the total fraction. Subsequent filtrations of the 10 mg/L H-cement were then immediately performed at 0.2 µm, followed by 10 kDa (Amicon® Ultra-4 3 K centrifugal filter devices (10 000MWCO, size retention limit ~ 2 nm, Merck-Millipore, 4000*g*, 30 min). Cement particle transformation was evaluated at t0, 1h, 5h, 24h, 3d, and 28 d by preparing different samples for each time point. Figure 17 shows the Ca, Si, Al, and Ti concentrations measured in the total, <0.2 µm and soluble (<10kDa) fractions at each time point. Of note, since the Ti recovery was extremely low with the selected acid digestion protocol, we were only able to accurately analyse Ti in the soluble fraction (<10kDa), which doesn't require digestion prior to elemental analysis. The dashed line represents the expected concentration for a 10 mg/L suspension of H-cement.

Calcium was determined to be the best tracer for the H-cement particle transformation, with a 103 ± 9% recovery in the total fraction for all the tested time points. An immediate dissolution of ~50% of the calcium was observed, with the % dissolved Ca increasing to ~60% after 28d. Concerning Si, quantification was not possible in any of the fractions due to the high and variable background in the Volvic® water. Furthermore, due to the Al and Ti recoveries being <100% in the total fraction, we could only accurately confirm that there was no Al or Ti released into the soluble fraction (<10kDa).

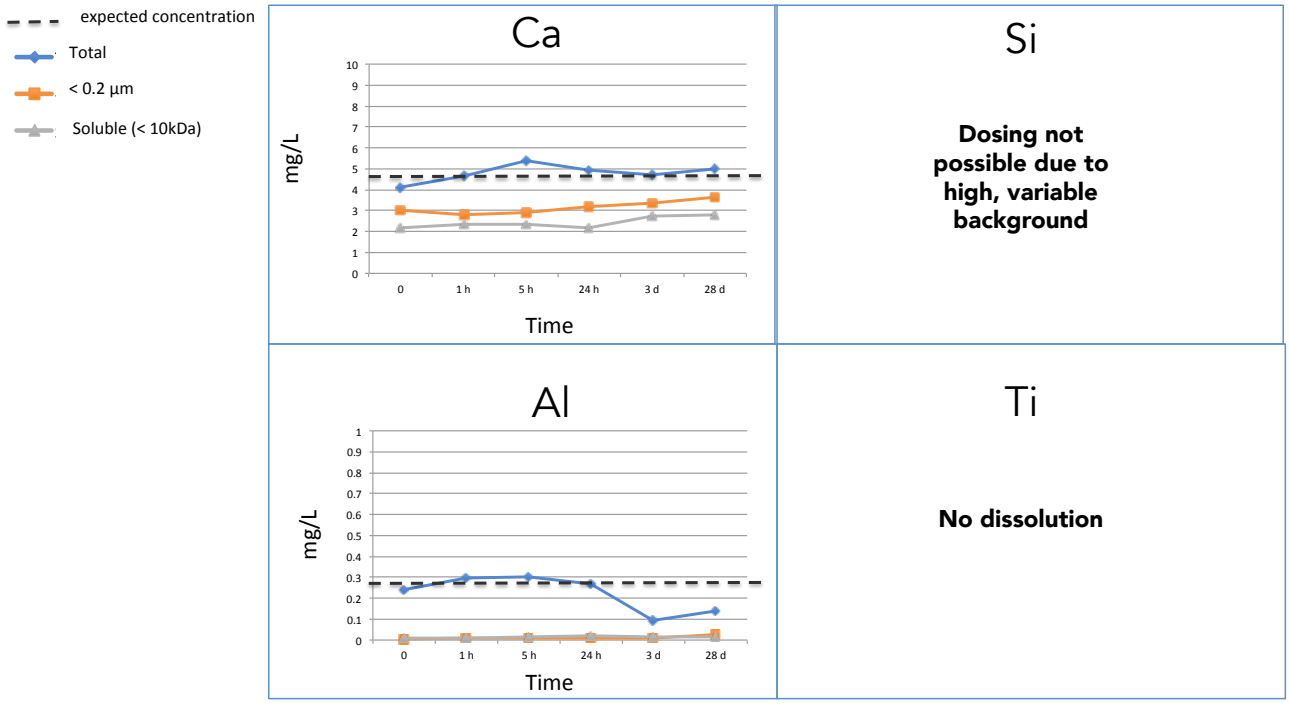

Figure 17. Ca, Si, Al, and Ti concentrations in different fractions over time for 10 mg/L H-cement suspension prepared in Volvic® water.

Since Ca was determined to be the best tracer for cement particle transformation, the Ca concentrations from each fraction were used to calculate the % of Ca remaining in the particulate (>0.2 µm), colloidal (0.002-0.2 µm), and soluble (<10kDa) fractions.

The % Ca in the soluble fraction was determined using the following equation:

$$\%\ soluble\ Ca\ = \frac{[Ca]soluble}{[Ca]total} \times 100\%$$

The % Ca in the colloidal fraction was determined using the following equation:

$$\%\ colloidal\ Ca\ = \left[\frac{[Ca] < 0.2\ um - [Ca]soluble}{[Ca]total}\right] \times 100\%$$

The % Ca in the particulate fraction was determined using the following equation:

$$\%\ particulate\ Ca\ = \frac{[Ca]total - [Ca] < 0.2um}{[Ca]total} \times 100\%$$

Figure 18 shows the changes in the % Ca in these fractions over time. As previously mentioned, ~50% of the Ca was immediately released into the soluble fraction, with the colloidal and particulate fractions making up ~15% and 35%, respectively. While the % colloidal fraction remained relatively stable over the 28d, the particulate fraction decreased from ~35 to 25%. This suggests that the Ca released into the Volvic® water resulted from dissolution directly from the particulate fraction.

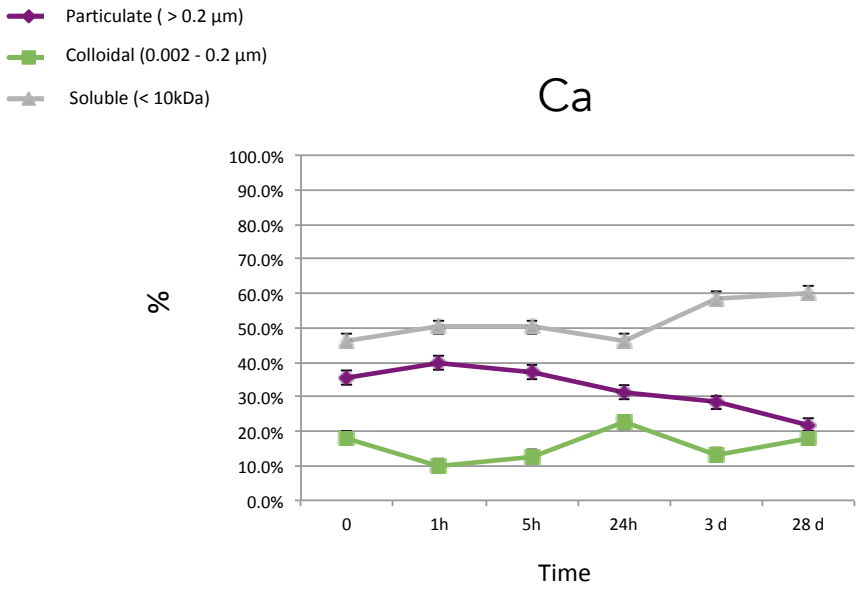

Figure 18. % Ca calculated for the particulate (>0.2 µm), colloidal (0.002-0.2 µm), and soluble (<10kDa) fractions after aging in Volvic® water.

Cement particle transformation was also investigated in non-contaminated water sampled from the aquatic mesocosms (Figure 19). Calcium was again the best tracer for the H-cement particle transformation, with a 98 ± 9% recovery in the total fraction for all the tested time points. Significant dissolution was immediately observed with ~50-70% being released into the soluble fraction over the 28d. In the mesocosm water, Si measurement was possible due to a lower background and the recovery was 98 ± 18%. Si was thus used as a secondary tracer for the cement particles. Furthermore, due to the Al and Ti recoveries being <100% in the total fraction, we could only accurately confirm that there was ~3-6% released into the soluble fraction (<10kDa) and that there was no Ti dissolution.

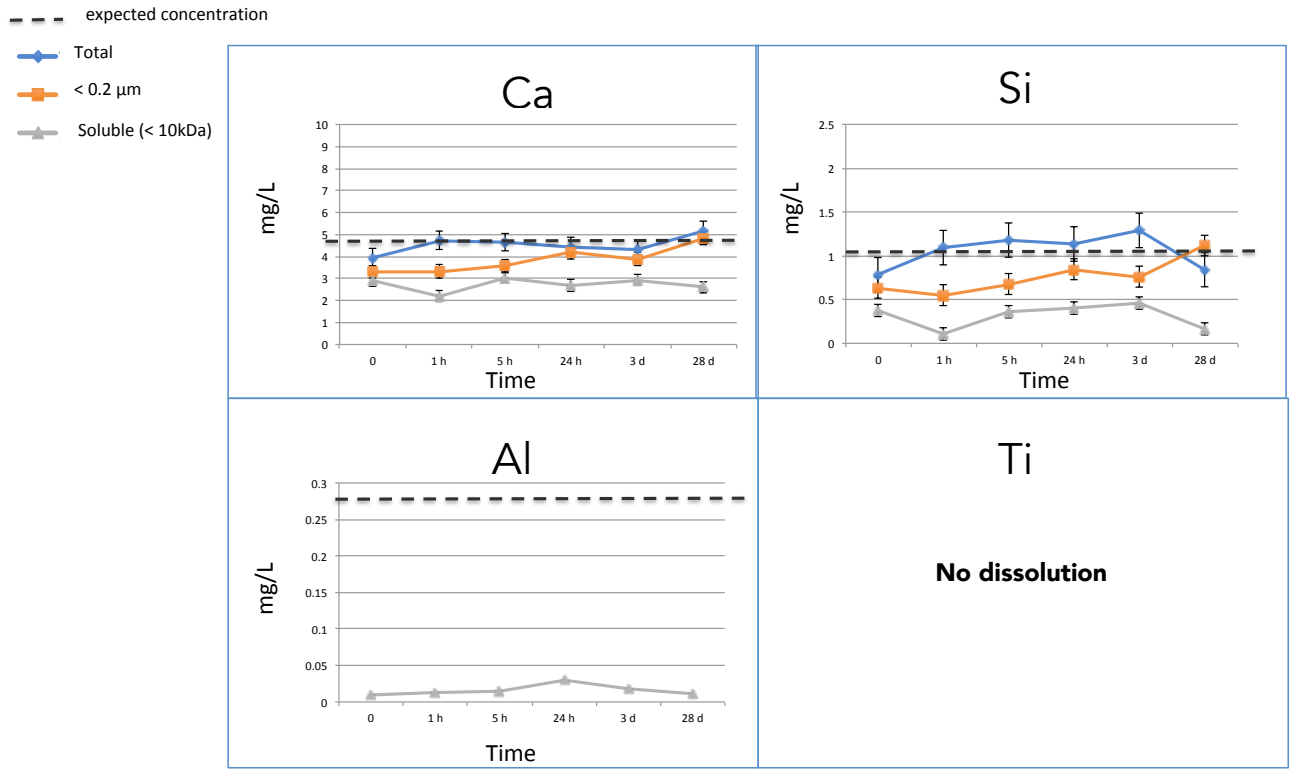

Figure 19. Ca, Si, Al, and Ti concentrations in different fractions over time for 10 mg/L H-cement suspension prepared in mesocosm water.

Figure 20 shows the changes in the % Ca and Si in the particulate (>0.2 µm), colloidal (0.002-0.2 µm), and soluble (<10kDa) fractions over time for H-cement in mesocosm water. With respect to the Ca, ~70 ± 5% of the Ca was immediately released into the soluble fraction, with the colloidal and particulate fractions making up ~10% and 16%, respectively. While the % Ca in the soluble fraction remained relatively stable, at the end of 28d the particulate fraction only represented ~7% and the %Ca in the colloidal fraction increased to 43%. These results show that a significant amount of Ca is immediately released into the soluble fraction of the mesocosm water, and after ~24h the >0.2 µm particles still present begin to fragment, releasing Ca-containing colloids. With respect to Si in the H-cement, ~30 ± 13% Si was measured in the soluble fraction during the 28d experiment, with a significant immediate release at t0. The particulate fraction represented ~20-40% of the total Si and the colloidal fraction was ~50-80% between t0 and 3d. After 28d of aging in the mesocosm water, the %Si in the colloidal fraction dramatically increased, representing almost the totality of the Si from the H-cement. Overall, these results from the batch experiments demonstrate a significant increase in the fraction of Ca- and Si-containing colloids after 28d. This observation is supported by the increase in the number of colloids measured with the optical counter at day 28 in Figure 16. Of note, with the Si concentrations being more variable, Ca was still deemed as the best tracer for the cement particles.

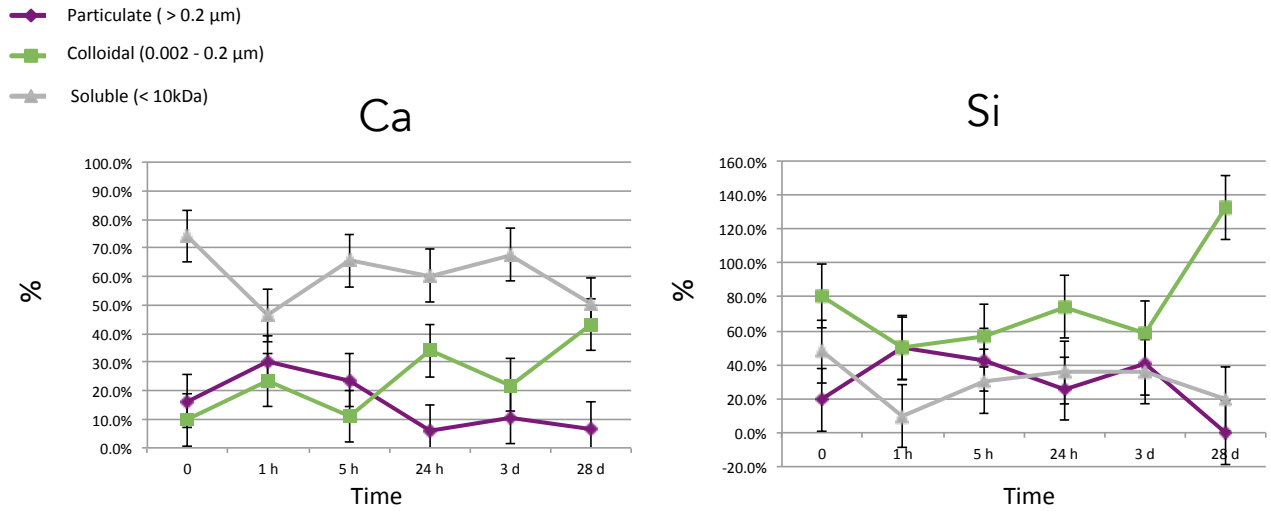

Figure 20. % Ca and Si calculated for the particulate (>0.2 µm), colloidal (0.002-0.2 µm), and soluble (<10kDa) fractions after aging in mesocosm water.

4.2 Estimated distribution in different environmental compartments

Using the data from section 3.1, we were able to estimate the potential distribution of the H-cement particles in the different environmental compartments of an aquatic mesocosm (water column, surficial sediment, primary consumers). At the end of 28d, ~50% of the Ca will be dissolved in the water column, ~40% will be present as colloids, and ~10% will be in particles >0.2 µm. Using Stokes law (as described in section 2.2.3), the settling times for the remaining colloids and particles were estimated using particle diameters of 0.2 µm and 2 µm, to represent the colloidal fraction and the initial cement particles, respectively. A particle of 2 µm was estimated to settle to the surficial sediment in ~20 h, however a colloid of ~0.2 µm could remain suspended in the water column for ~82 days. Unlike for the SS316L particles that settled out rapidly, both the planktonic and benthic compartments of the aquatic mesocosms will be exposed to the H-cement particles and by-products.

Ongoing work is being completed to understand how the transformation of tritiated cement particles will impact the distribution of tritium in the aquatic ecosystem. The tritium dose in the surficial sediments can be dosed after exposure to the tritiated cement particles (T-cement), but due to the high environmental background of all relevant elements in the sediment, we are unable to detect, dose, and trace the cement particles in the surficial sediments, even if 100% of the cement was to settle down (with no transformation). Table 4 shows the background concentrations of major and trace elements in the surficial sediments, along with the potential added concentrations from a contamination of 10 mg/L cement particles. Studying a higher concentration of cement particles (i.e., >10 mg/L) for these environmental fate studies was not pursued because the higher contamination concentrations would not be environmentally relevant.

Table 4. Estimation of cement particle concentration that can be detected and quantified in mesocosm surficial sediments, assuming all cement settles to sediment.

Element	Background in sediment (ug/g)	10 mg/L cement addition (ug/g)	Detection possible?
Ca	40961 ± 7244	1109	X
Si	220635 ± 6855	259	X
Al	6685 ± 322	64.5	X
Ti	3318 ± 82	41.6	X
Fe	29260 ± 526	5.1	X
Cr	61.7 ± 1.1	0.2	X
Ni	38.1 ± 0.7	0.13	X
Cd	0.36 ± 0.03	0.0096	X
Cu	52.7 ± 0.4	0.0478	X
Zn	111.3 ± 4.7	0.203	X

The potential interactions of the cement particles with the primary consumers (i.e., benthic grazers) in the aquatic mesocosms were also considered. As with the surficial sediments, the elevated background concentrations of the relevant major and trace elements prevent the tracing of the cement particles and by-products in the *A. leucostoma* (Table 5). Table 5 shows that even in the best-case scenario where the cement particles are not transformed and A. leucostoma (~0.005%) uptake is comparable to that of the SS316L particles, none of the relevant elements present in cement can be used as a tracer. However, ongoing work is being completed to evaluate the tritium uptake in these organisms after exposure to T-cement particles.

Table 5. Estimation of cement particle concentration that can be detected and quantified in A. leucostoma, assuming no cement transformation and comparable uptake to SS316L particles.

Element	Background in snails (mg/kg)	10 mg/L cement addition (mg/kg)	Detection possible?
Ca	2.70E+05	18.6	X
Si	X	4.3	X
Al	1.9 ± 2.3	1.08	X
Ti	18.5 ± 5.2	0.696	X
Fe	826.1 ± 358.3	0.085	X
Cr	0.42 ± 0.17	0.0027	X
Ni	0.58 ± 0.07	0.0022	X
Cd	0.41 ± 0.03	0.0002	X
Cu	2.96 ± 0.21	0.0008	X
Zn	12.70 ± 1.0	0.0034	X

5 Conclusions

The present indoor freshwater mesocosm set-up and complementary batch experiments performed permit the analysis of the environmental fate and impact of both tritiated by-products and dissolved tritium. Our results highlight drastic differences in the contamination routes of a freshwater ecosystem and differences in the ecological niches potentially exposed to tritiated (^{3}H) steel or cement particles released during dismantling. Indeed, the stainless steel particles were stable, but rapidly settled out of the water column. Only a small fraction of the tritium was released into the water column in the dissolved phase. The majority of the tritium remained bound to the steel particles residing in the surficial sediments. Benthic grazers appeared particularly sensitive to the stainless steel particles with significant behavioural changes observed. In the case of cement, there is an immediate dissolution of the particles, which will surely coincide with an important release of tritium in the water column. In that case we expect a more important exposure of the planktonic organisms to ^{3}H.

Freshwater indoor mesocosms appeared as well adapted experimental devices to quantitatively and qualitatively assess environmental dosimetry and the impacts of tritiated steel and cement particles likely released in aquatic ecosystems during dismantling.

6 Cited references

Auffan, M., Liu, W., Brousset, L., Scifo, L., Pariat, A., Sanles, M., et al. (2018). Environmental exposure of a simulated pond ecosystem to CuO nanoparticle based-wood stain throughout its life cycle. *Environmental Science: Nano* 5, 2579–2589. doi:10.1039/C7EN00494J.

Auffan, M., Masion, A., Mouneyrac, C., de Garidel-Thoron, C., Hendren, C. O., Thiery, A., et al. (2019). Contribution of mesocosm testing to a single-step and exposure-driven environmental risk assessment of engineered nanomaterials. *NanoImpact* 13, 66–69. doi:https://doi.org/10.1016/j.impact.2018.12.005.

Auffan, M., Santaella, C., Brousset, L., Tella, M., Morel, E., Ortet, P., et al. (2020). The shape and speciation of Ag nanoparticles drive their impacts on organisms in a lotic ecosystem. *Environmental Science-Nano*, 3167–3177.

Auffan, M., Tella, M., Santaella, C., Brousset, L., Pailles, C., Barakat, M., et al. (2014). An adaptable mesocosm platform for performing integrated assessments of nanomaterial risk in complex environmental systems. *Scientific reports* 4, 5608.

Ayadi, A., Rose, J., de Garidel-Thoron, C., Hendren, C., Wiesner, M. R., and Auffan, M. (2021). MESOCOSM: A mesocosm database management system for environmental nanosafety. *NanoImpact* 21, 100288. doi:10.1016/j.impact.2020.100288.

Chatel, A., Auffan, M., Perrein-Ettajani, H., Brousset, L., Metais, I., Chaurand, P., et al. (2020). The necessity of investigating a freshwater-marine continuum using a mesocosm approach in nanosafety: the case study of TiO2 MNM-based photocatalytic cement. *Nano impact*, 100245.

Lillebø, A. I., Pardal, M. Â., and Marques, J. C. (1999). Population structure, dynamics and production of Hydrobia ulvae (Pennant) (Mollusca: Prosobranchia) along an eutrophication gradient in the Mondego estuary (Portugal). *Acta Oecologica* 20, 289–304. doi:https://doi.org/10.1016/S1146-609X(99)00137-X.

MacInnes, J. R., and Thurberg, F. P. (1973). Effects of metals on the behaviour and oxygen consumption of the mud snail. *Marine Pollution Bulletin* 4, 185–186. doi:https://doi.org/10.1016/0025-326X(73)90225-7.

Masion, A., Auffan, M., and Rose, J. (2019). Monitoring the Environmental Aging of Nanomaterials: An Opportunity for Mesocosm Testing? *Materials* 12, 2447.

Nassar, M., Auffan, M., Santaella, C., Masion, A., and Rose, J. (2020). Multivariate Analysis of the Exposure and Hazard of Ceria Nanomaterials in Indoor Aquatic Mesocosms. *Environmental Science: Nano*, 1661–1669.

Nassar, M., Auffan, M., Santaella, C., Masion, A., and Rose, J. (2021). Robustness of Indoor Aquatic Mesocosm Experimentations and Data Reusability to Assess the Environmental Risks of Nanomaterials. *Frontiers in Environmental Science* 9, 176. doi:10.3389/fenvs.2021.625201.

Roell, K. R., Reif, D. M., and Motsinger-Reif, A. A. (2017). An Introduction to Terminology and Methodology of Chemical Synergy-Perspectives from Across Disciplines. *Front Pharmacol* 8, 158. doi:10.3389/fphar.2017.00158.

Tella, M., Auffan, M., Brousset, L., Issartel, J., Kieffer, I., Pailles, C., et al. (2014). Transfer, transformation and impacts of ceria nanomaterials in aquatic mesocosms simulating a pond ecosystem. *Environmental Science & Technology* 48, 9004–9013.

Tella, M., Auffan, M., Brousset, L., Morel, E., Proux, O., Chaneac, C., et al. (2015). Chronic dosing of a simulated pond ecosystem in indoor aquatic mesocosms: fate and transport of CeO2 nanoparticles. *Environmental Science: Nano* 2, 653–663.

7 Annexes

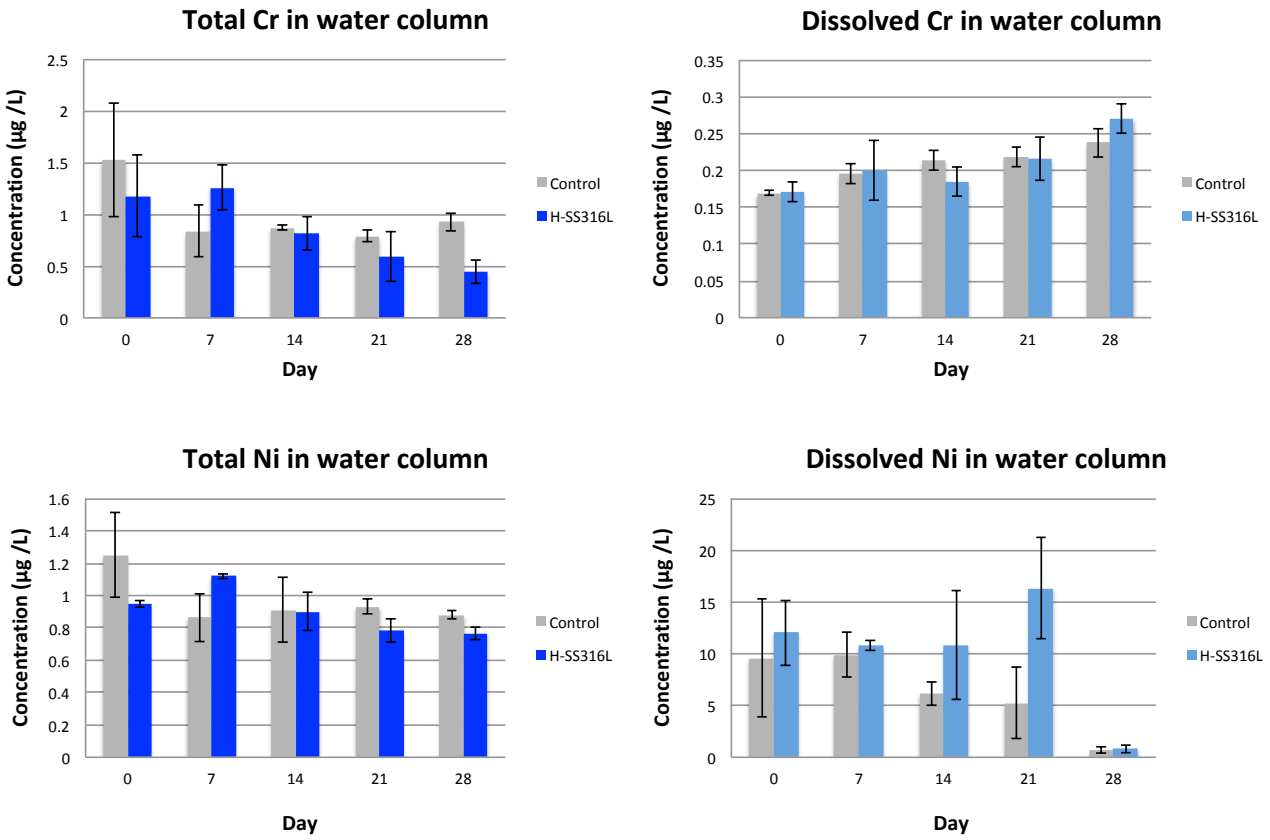

Figure A 1. Total and dissolved concentrations of Cr and Ni in water column.

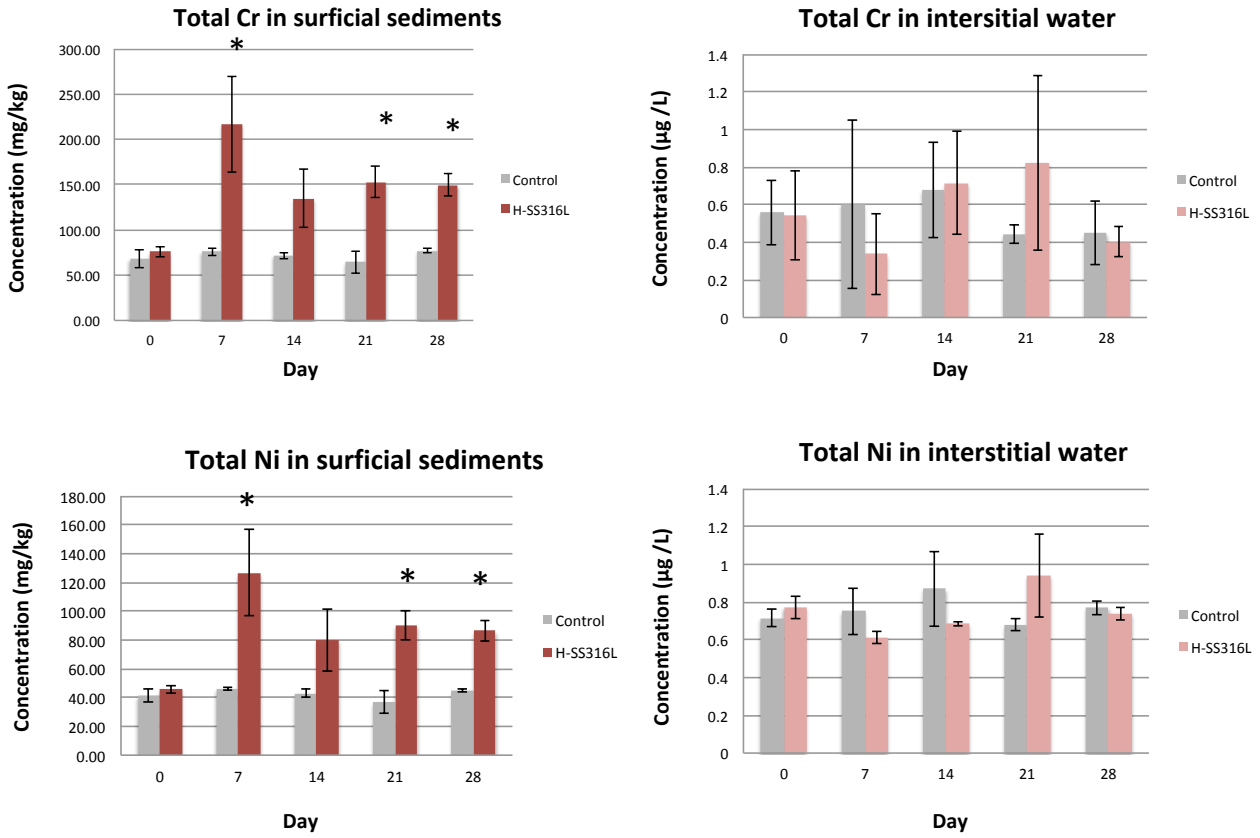

Figure A 2. Total concentrations of Cr and Ni in surficial sediments and interstitial water.

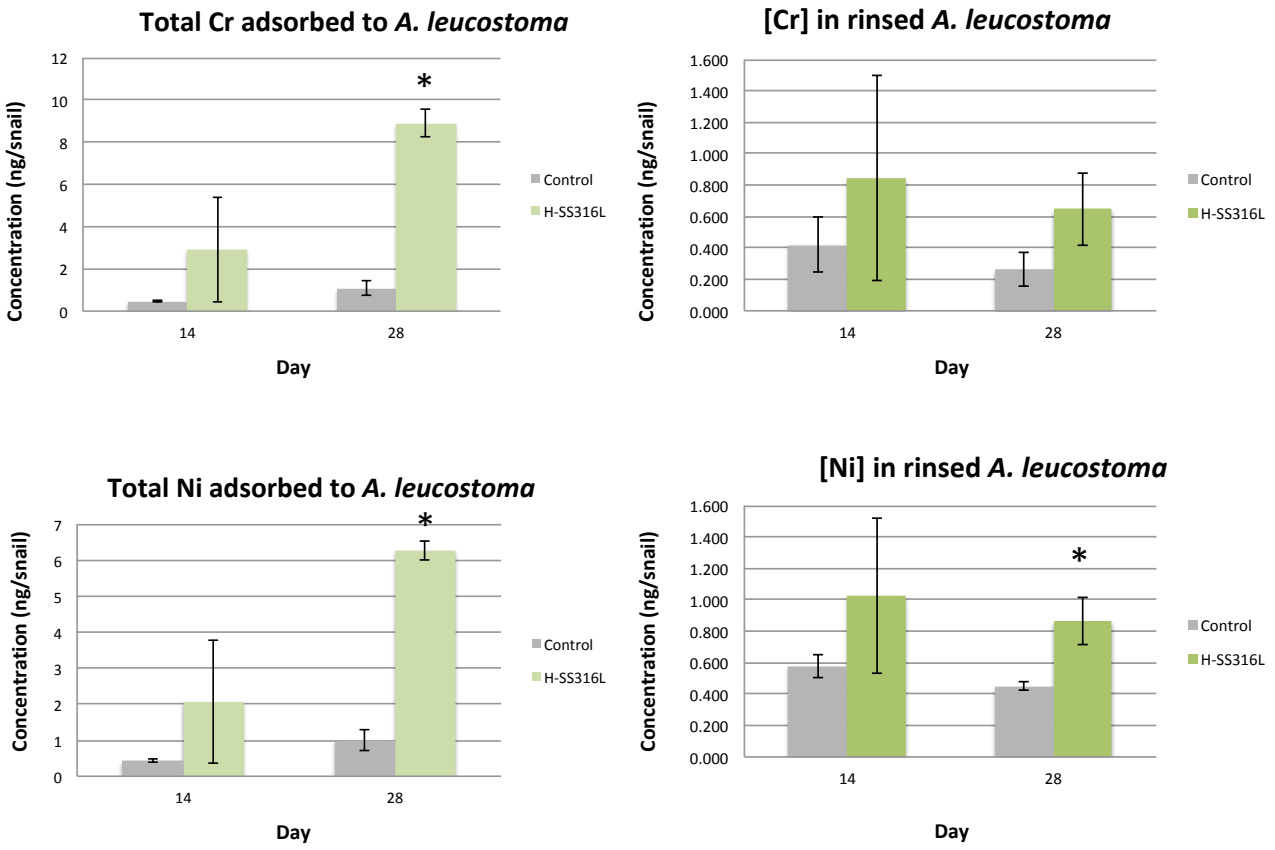

Figure A 3. Total concentrations of Cr and Ni adsorbed to (left) and taken up in snails (right).